The Effects of Late Spring Frost on Forest and Landscape Health of the Black Rock Forest, New York

CAROLINE ECO[1], OLIVER IMHANS[2],

AARON DAVITT[3], ANDREW B. REINMANN[4,5]

CREST Research Experience for Undergraduate Program
[1] Electrical Engineering Technology Department, New York City College of Technology, CUNY
[2] Department of Mathematics, New York City College of Technology, CUNY
[3] The Graduate Center, CUNY
[4] Environmental Sciences Initiative, CUNY Advanced Science Research Center
[5] Department of Geography and Environmental Science, Hunter College

ABSTRACT

Projected changes in climate are expected to increase the frequency of late spring frost events in the Northeast US. Such events can be harmful to trees because freezing temperatures that occur after leaf-out can damage or kill young leaves. The resultant defoliation typically forces a second flush of leaves, but delays canopy development, which in turn delays the onset of canopy carbon uptake and alters canopy thermal properties. While forest response to defoliation events has been studied, much of this work has focused on insect-driven events (e.g., gypsy moth), which often occur later in the season and likely have different ecological implications than spring frost-induced defoliation events. Here, we use satellite-based remote sensing analyses to study the impacts of spring frost-induced defoliation on canopy green-up dynamics in a temperate deciduous forest.

In this study, we analyzed a recent freeze event that occurred on May 8-9, 2020 (DOY 129-130) at Black Rock Forest (BRF), which is located in the Hudson Highlands of southeastern New York State. We compared satellite images collected during the 2019 (no frost) and 2020 growing season. The purview of this analysis includes: 1. A comparison of the current year to the previous year to determine the productivity of forest ecosystems and their ability to bounce back after the frost. 2. The impact of the frost event on landscape thermal properties by comparing growing season land surface temperature between the year with the frost event (i.e. 2020) to previous year (i.e. 2019).

We use the Landsat-8 Normalized Difference Vegetation Index (NDVI) to assess spatial and temporal patterns in canopy development. The land surface temperature (LST) is used to measure the temperature of the forest before and after the frost. The mean results of the NDVI value from Landsat-8 data highlights the differences in the timing of greenness between the two years. After DOY 129-2019 and DOY 130-2020, there is a decrease in NDVI for 2020 which suggests a delay in the canopy development. Analyses of ECOsystem Spaceborne Thermal Radiometer Experiment (ECOSTRESS) imagery indicates a rise in LST after 9 May 2020. LST patterns after 9 May 2019 are higher than that of 2020 from mid-May to early June. The mean LST of low elevation forests which did not defoliate shows that higher elevation is hotter than other locations.

Keywords: Frost, Black Rock Forest (BRF), Hudson Highlands, New York, Landsat-8, land surface temperature (LST), Normalized Difference Vegetation Index (NDVI), ECOsystem Spaceborne Thermal Radiometer Experiment (ECOSTRESS)

1. INTRODUCTION

Frost is the occurrence of subfreezing temperatures that causes atmospheric moisture to directly crystallize unto exposed objects [Rafferty, 2019]. The presence of late spring frosts, combined with warm winters, provoke damaging effects to tree health. Warmer winters trigger some trees to bud burst early which makes them more vulnerable to frost damages [Augspurger, 2009]. Projected changes in climate such as this are expected to lengthen the growing season of trees in the Northeast US with an increased likelihood of late frosts in springtime. [Hayhoe et al., 2006] Such events can be harmful to trees because when frost forms inside premature buds and leaves, the young leaves get damaged [Augspurger, 2013]. The resultant defoliation from late spring frosts typically forces a second flush of leaves when adventitious buds are triggered to bud burst. In temperate deciduous forests, hard freezes negatively affect the apical meristems of trees which contributes to the structure of the canopy. [Vitasse et al., 2014] This re-foliation further delays the onset of canopy carbon uptake and alters canopy thermal properties. While forest response to defoliation events has been studied, much of this work has focused on insect-driven events (e.g., gypsy moth), which often occur later in the season and likely have different ecological implications than spring frost-induced defoliation events. Here, we use satellite-based remote sensing analyses, along with field measurements, to study the impacts of spring frost-induced defoliation on canopy green-up dynamics in a temperate deciduous forest.

This study is an analysis of the recent freeze event that occurred on 8-9 May 2020 (DOY 129-2020-DOY 130-2020) at Black Rock Forest (BRF). We compared satellite images collected in 2019, where there was no late spring frost event, and in 2020, before and after the frost event. We use the Landsat-8 Normalized Difference Vegetation Index (NDVI) to assess spatial and temporal patterns in canopy development. The land surface temperature (LST) is used to measure the temperature of the forest before and after the frost. The mean results of the NDVI value from Landsat-8 data highlights the differences in the timing of greenness between the two years. This allows us to define the effects of the frost event on the formation of the canopy. After 9 May 2020, there is a stark decrease in NDVI which suggests a delay in the canopy development. During this time, analyses of ECOsystem Spaceborne Thermal Radiometer Experiment (ECOSTRESS) imagery indicates a rise in LST with warmer temperatures compared to that of 2019. Our field measurements indicate that the mean LST of low elevation forests, which did not defoliate, shows that higher elevation is hotter than other locations. In mid-May of 2020, a PhenoCam was installed in Fire Tower Station, one of the field stations in BRF (See Figure 2a). PhenoCam images show the absence of greenness and confirm the low NDVI values right after the frost event (See Figure 2B). It also shows that forest recovery started appearing approximately 20 days after the frost event (See Figure 2c).

The purview of this analysis includes: 1. A comparison of the current year to the previous years to determine the productivity of forest ecosystems and their ability to bounce back after the frost. 2. The impact of the frost event on landscape thermal properties by comparing growing season land surface temperature between the year with the frost event (i.e. 2020) to the previous year.

The objectives of this research are to: 1. Investigate the Landsat-8 Normalized Difference Vegetation Index (NDVI) to assess spatial and temporal patterns in canopy development. 2. Use the Land Surface Temperature (LST) to measure the temperature of the forest before and after the frost. 3. Use the mean results of the NDVI value from Landsat-8 data and Land Surface Temperature (LST) to highlight the differences in the timing of greenness between the two years. 4. Use Ecosystem Spaceborne Thermal Radiometer Experiment (ECOSTRESS) imagery for further analysis of forest health and LST variability within BRF.

The end goals are to: 1. Produce datasets that measure tree health and vegetation growth responses based on Landsat-8 NDVI 2. Produce datasets that measure the land surface temperature (LST) using the ECOSTRESS sensor to assess landscape health.

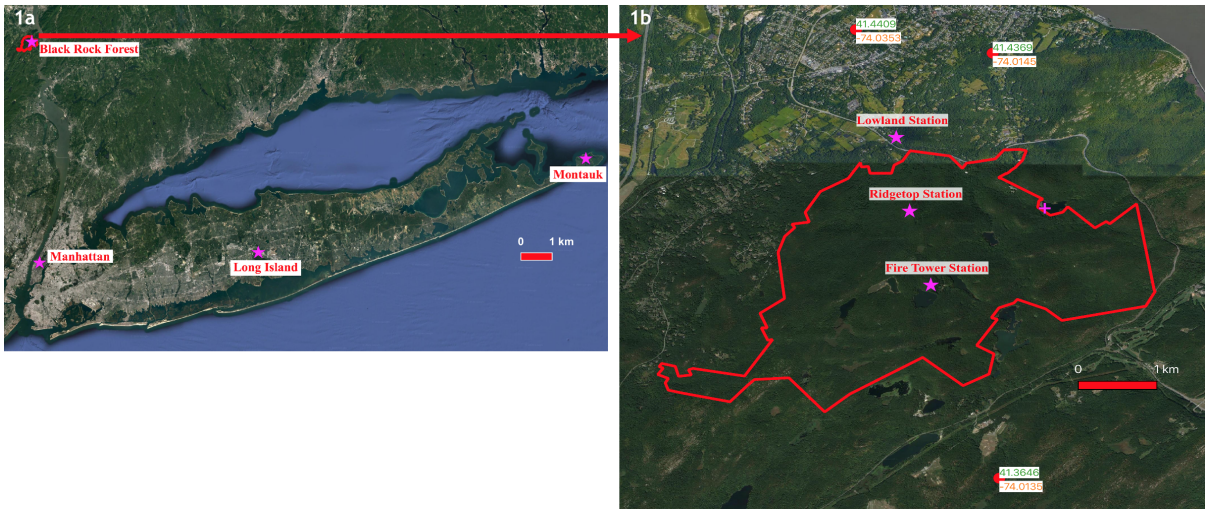

Figure 1. a) Google Earth image with a red polygon marking Black Rock Forest and pink stars marking Manhattan, Long Island and Montauk b) Google Earth close-up of Black Rock Forest with pink stars marking Lowland Station, Ridgetop Station and Fire Tower Station, and a cross marking Hill of Pines trailhead. The red dots mark points of latitude, in green font, and longitude, in orange font

2. METHODS

The research project centers on Black Rock Forest, a landmass that covers about 3,870-acre (15.7 km^2) of the biological field station and forest located in the Hudson Highlands of southeastern New York State (See Figure 1a-1b). Two different approaches were used for analysis: 1. The Normalized Difference Vegetation Index (NDVI) 2. The Land Surface Temperature (LST). Field measurements to support the NDVI findings are provided by the PhenoCam network (Figure 2a-2c). Field measurements to support the LST findings are provided by weather station data and sensors installed on Fire Tower Station in BRF (Figure 3a-3c). Frost damages on young oak leaves and flowers were captured in images taken on 16 May 2020 at the Hill of Pines trailhead (See Figure 4a-4c).

Figure 2. a) Phenocam installed on Fire Tower Station of Black Rock Forest b) Phenocam image taken on 17 May 2020, highlighting a dry and damaged forest after the late spring frost c) Phenocam image taken on 22 May 2020, highlighting forest recovery nine days after the frost event

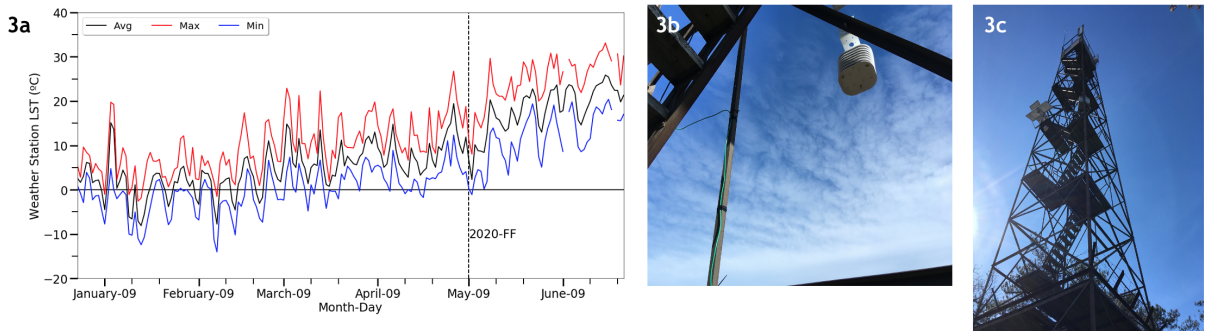

Figure 3. a) Weather station data indicating the late spring frost on 9 May 2020 b-c) Temperature sensor installed on Fire Tower Station in Black Rock Forest

Figure 4. a) View from Hill of Pines trailhead on 16 May 2020. All red and black oaks seem to have suffered damage from the freeze, keeping things looking like early spring. The presence of leaves is possibly evidence of a second flush in its early stages b) Oak flowers and c) young oak leaves killed by the 2020 freeze event Images taken on 16 May 2020

2.1 Landsat-8, NDVI, ECOSTRESS, LST

Landsat-8 is an orbital satellite that provides moderate-resolution (15 m–100 m, depending on spectral frequency) measurements of the Earth's terrestrial and polar regions in the visible, near-infrared, short wave infrared, and thermal infrared. It uses Operational Land Imager (OLI) and Thermal Infrared Sensors (TIRS) to return 400 scenes per day to the United States Geological Survey (USGS) data archive. Landsat-8 provides Near-Infrared (IR) and Red (R) band readings for calculation of the Normalized Difference Vegetation Index (NDVI).

NDVI is a measurement of the health state of the plant. This measurement is based on how plants reflect different wavelengths of light in the electromagnetic spectrum. During measurements, some waves are absorbed, while others are reflected. As an example, "Chlorophyll a healthy plant indicator strongly absorbs visible light, while on the other hand, the cellular structure of the leaves reflects strongly near-infrared light" [Verhoeven, 2011]. NDVI is used as a quantifier for vegetation greenness, which is useful in

discerning changes in plant health and vegetation density. It is a benchmark of vegetation health because a decrease in a forest's natural greenness would be reflected in a decrease in its NDVI value.

Measurements results from NDVI are within the range of -1 to 1, where the negative values infer areas with water-related surfaces. According to the USGS, "NDVI values range from +1.0 to -1.0. Areas of barren rock, sand, or snow usually show very low NDVI values (for example, 0.1 or less). Sparse vegetation such as shrubs and grasslands or senescing crops may result in moderate NDVI values (approximately 0.2 to 0.5). High NDVI values (approximately 0.6 to 0.9) correspond to dense vegetation such as that found in temperate and tropical forests or crops at their peak growth stage".

NDVI is calculated as a ratio between the red (R) and near infrared (NIR) values:

$$\text{NDVI} = \frac{NIR - RED}{NIR + RED}$$

Where NIR is the near infrared values from Landsat-8 data in Band 5, and RED is the values from Landsat-8 data in Band 4. For the purpose of this project, measurements results from NDVI are within the range of 0 to 1.

ECOSTRESS is a sensor aboard the International Space Station (ISS). It measures the thermal infrared brightness temperatures (BT) of plants for the purposes of defining evapotranspiration, the evaporation and transpiration of vegetation, and describing the earth's land surface temperature. It has a multispectral scanner with three thermal infrared (TIR) bands (8.0 – 12.5 μm, mid- to long-wave IR) with an approximately 70m spatial resolution. Its orbital path enables it to gather 46.6 sweeps of data per minute or an average of 1 hour of data science per day.

LST measurements provide information on landscape thermal properties. LST images highlight warmer temperatures on urban areas compared to areas with vegetation (See Figure 10a). LST is also useful in highlighting bodies of water (See Figure 11b). Since water temperature is significantly more stable compared to land, which tends to cool off in the absence of sunlight, the LST of bodies of water record warmer temperatures. We compared the ECOSTRESS LST data to Landsat-8 NDVI measurements between the two years to assess the impact of the frost event and determine what is the corresponding LST with respect to NDVI.

We downloaded satellite data collected by the Landsat-8 satellite and the ECOSTRESS sensor from the National Aeronautics and Space Administration (NASA) - Application for Extracting and Exploring Analysis Ready Samples (AρρEEARS) website from January to July for 2019 and 2020. We used the python graphical user interface (gui), Anaconda Navigator, for three programs that: 1. create cloud-free images by creating a cloud mask and filtering out the cloudy pixels from the raw satellite data. 2. extract statistical data from the raw data frames and 3. formulate time series plots for the NDVI and LST (See Figures 8a-8b and Figures 12a-12c). We loaded the cloud-free images in the Quantum Geographic Information System (QGIS) software and used the Raster tool to create the NDVI images and difference images for NDVI and LST. This was done to make a comparison of the current year to the previous years to determine the productivity of forest ecosystems and their ability to bounce back after the frost; and to assess spatial and temporal patterns in canopy development. The timing of greenness between the two years, forest health, and LST variability will be analyzed.

3. Analysis

3.1 NDVI Analysis

NDVI sensitivity to low and high growth stages (See Figure 5a-5b) portrays the low disparity in growth for years 2019 and 2020 before the date of the frost event. The sensitivity analysis of NDVI from 0

to 1 in order of magnitude reveals areas of arid land, sand, or snow that usually show very low NDVI values. Scanty vegetations and grasslands may lead to moderate NDVI values. The high NDVI values correlate to thick vegetation or crops at their peak stage of growth.

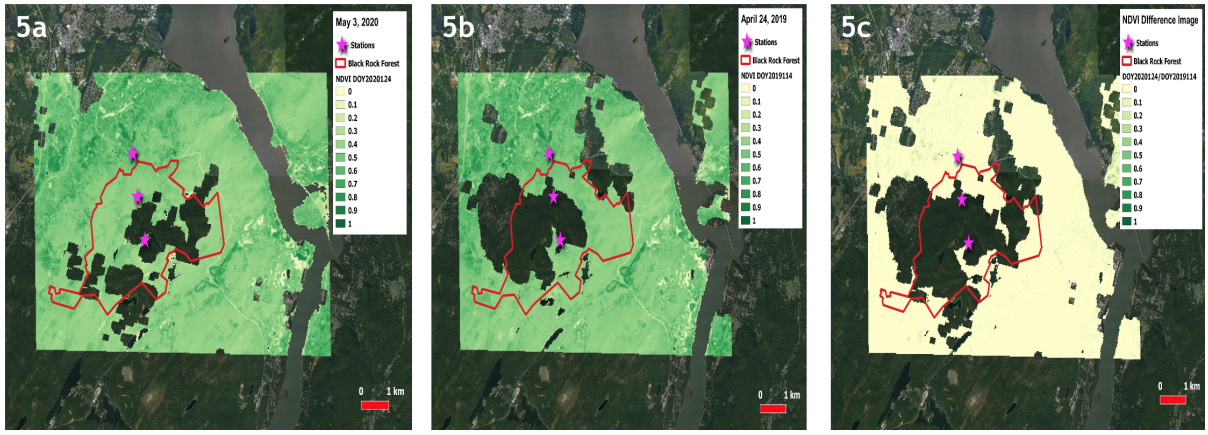

Figure 5. a) NDVI image for 3 May 2020 before the late spring frost b) NDVI image for 24 April 2019 highlighting similar forest greenness to Figure 5a c) NDVI difference image (3 May 2020 - 24 April 2019)

Similarly, the same sensitivity to low and high growth (See Figure 6a-6b) portrays a large disparity in growth for years 2019 and 2020 after the frost event in 2020. Frost damages are reflected on the NDVI image on 12 May 2020 highlighting a stark absence of greenness right after the late spring frost. The complete wipeout of all greenness symbolizes the negative effect of the frost event to canopy vegetation. A PhenoCam image taken on 17 May 2020 confirms our NDVI findings and shows a severely affected forest (See Figure 2b).

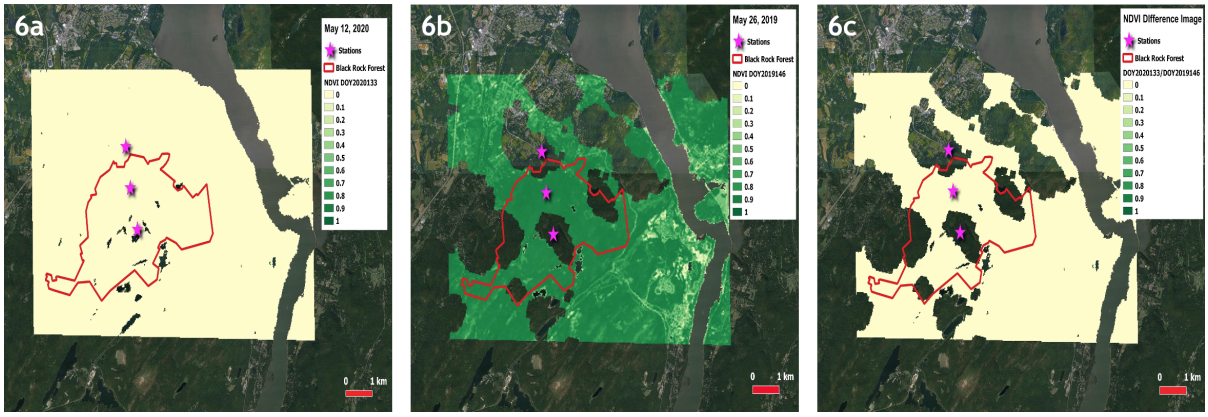

Figure 6. a) NDVI image for 12 May 2020 right after the late spring frost highlighting the absence of greenness and the frost damages b) NDVI image for 26 May 2019 highlighting close to peak levels of forest growth c) NDVI difference image (12 May 2020 – 26 May 2019)

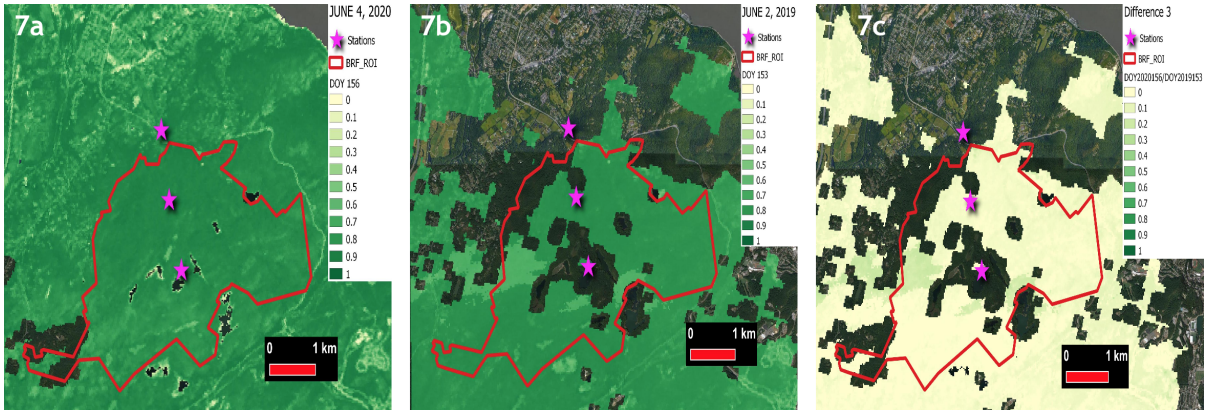

Figure 7. a) NDVI image for 4 June 2020 highlighting forest recovery from the frost event b) NDVI image for 2 June 2019 showing a healthy forest in 2019 c) NDVI difference image (4 June 2020 – 2 June 2019)

3.1.1 NDVI Patterns

NDVI patterns show us the health of the forest and how it is affected by the frost event. The NDVI in 2019 reflects the growing season of BRF without the interference of a late spring frost (See Figure 8a). It starts from the lowest mean NDVI value of 0.14 on 7 March 2019 and peaks at a highest mean NDVI value of 0.87 on 26 May 2019 (See Table 1). The NDVI in 2020 reflects a stagnant forest with mean NDVI values ranging from 0.30-0.43 from 22 February to 3 May 2020 (See Table 1). It then picks up with a mean NDVI value of 0.83 on 4 June 2020. This rise in NDVI represents forest recovery with a higher level of greenness. A PhenoCam image taken on 22 May 2020 confirms our NDVI findings and the forest recovery of BRF (See Figure 2c).

3.1.2 NDVI and Elevation

Field measurements from the three stations indicate a higher NDVI reading from the Lowland Station from mid-March towards the end of April. Low NDVI readings from the Fire Tower Station are shown around mid-February to mid-March. The significant decrease in NDVI from the Fire Tower Station from mid-June to mid-July suggests a correlation between NDVI and elevation, specifically in BRF. Further observations are required to confirm this observation. (See Figure 8b).

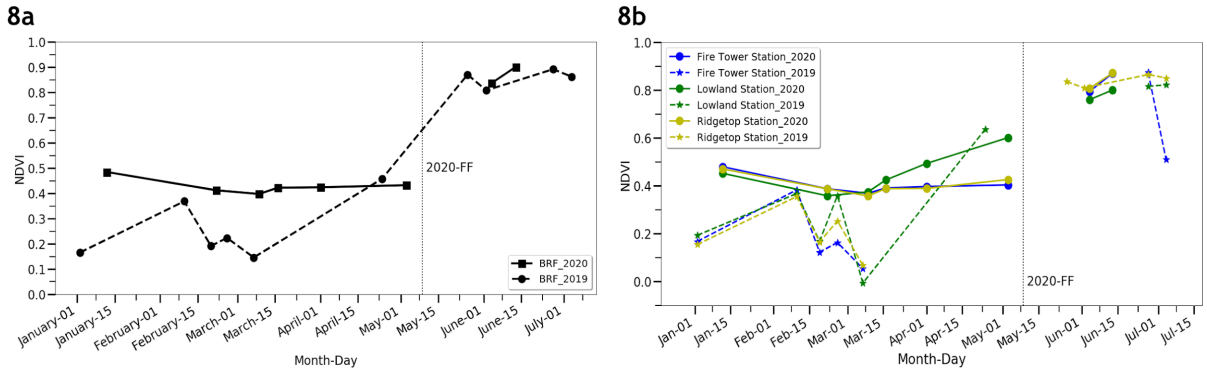

Figure 8. a) Comparison of NDVI of Black Rock Forest between 2020 and 2019 b) Landsat-8 mean NDVI values taken at the Lowland, Ridgetop and Fire Tower Stations from January to mid-July for years 2020 and 2019

Table 1. *Landsat-8 NDVI Statistics of Black Rock Forest for years 2020 and 2019*

Data number	Pixel count	Minimum NDVI	Maximum NDVI	Mean NDVI	std	Year	DOY	Date
0	24154	-0.8	0.8418722	0.48489887	0.0776744	2020	12	12-Jan-2020
1	24154	-0.4759358	0.74730355	0.41218904	0.08049704	2020	53	22-Feb-2020
2	24154	0.11145038	0.61556065	0.39749756	0.04789872	2020	69	9-Mar-2020
3	24154	-0.4142857	0.73706895	0.42228696	0.07098936	2020	76	16-Mar-2020
4	24154	-0.7714286	0.752357	0.42416286	0.07376547	2020	92	1-Apr-2020
5	24154	0.11068335	0.80087376	0.43244952	0.05584279	2020	124	3-May-2020
7	24154	0.10854207	0.9131044	0.8372111	0.0552058	2020	156	4-Jun-2020
8	24154	0.14285715	0.9476992	0.9012141	0.04084336	2020	165	13-Jun-2020

Data number	Pixel count	Minimum NDVI	Maximum NDVI	Mean NDVI	std	Year	DOY	Date
0	24154	0.04889179	0.27904668	0.16550137	0.02569236	2019	2	2-Jan-2019
1	24154	-0.380684	0.6603774	0.36869225	0.08469847	2019	41	10-Feb-2019
2	24154	-0.1433945	0.98613036	0.19165827	0.09491737	2019	50	19-Feb-2019
3	24154	-0.2887286	0.796875	0.22352433	0.11721768	2019	57	26-Feb-2019
4	24154	-0.1641642	1	0.14582348	0.15304184	2019	66	7-Mar-2019
5	24154	0.19316968	0.7560031	0.45779482	0.05128758	2019	114	24-Apr-2019
6	24154	0.3033033	0.972352	0.87081325	0.04072584	2019	146	26-May-2019
7	24154	0.54252607	0.8661877	0.80824727	0.04767034	2019	153	2-Jun-2019
8	24154	-0.9879518	0.96594095	0.8921331	0.07920764	2019	178	27-Jun-2019
9	24154	-0.6788321	0.9888716	0.86227244	0.10514198	2019	185	4-Jul-2019

3.2 LST Analysis

3.2.1 LST Comparisons and Difference Images

LST readings are lower on 21 May 2020 compared to 25 May 2019, showing a cooler forest (See Figure 9a and 9b). The LST variation of 10-13ºC (See Table 2) between 21 May 2020 and 25 May 2019 is depicted in a difference image (See Figure 9c). LST readings are higher on 13 June 2020 compared to 13 June 2019, showing a warmer forest (See Figure 10a and 10b). The LST variation of 7-17ºC (See Table 2) between 13 June 2020 and 13 June 2019 is depicted in a difference image (See Figure 10c). LST readings are higher on 21 June 2020 compared to 27 June 2019, showing a much warmer forest (See Figure 11a and 11b). The LST variation of 17-20ºC (See Table 2) between 21 June 2020 and 27 June 2019 is depicted in a difference image (See Figure 11c). The anomalies in LST between the two years could also be attributed to the timing when the images were taken by the sensor.

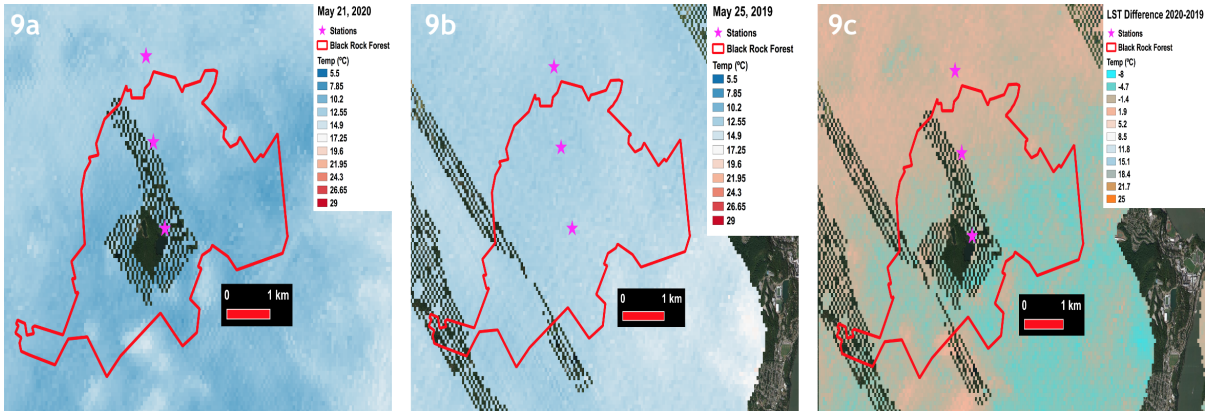

Figure 9: a) LST on 21 May 2020, local time 8:08pm b) LST on 25 May 2019, local time 6:50pm c) LST difference image (21 May 2020 - 25 May 2019) with a temperature difference scale ranging from -8° to 25°

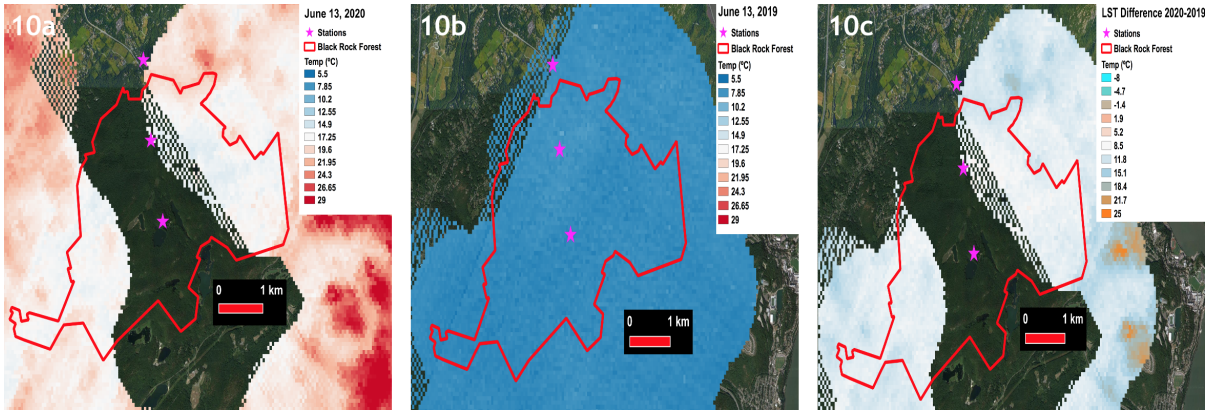

Figure 10: a) LST on 13 June 2020, local time 10:40am b) LST on 13 June 2019, local time 5:43pm c) LST difference image (13 June 2020 – 13 June 2019) with a temperature difference scale ranging from -8° to 25°C

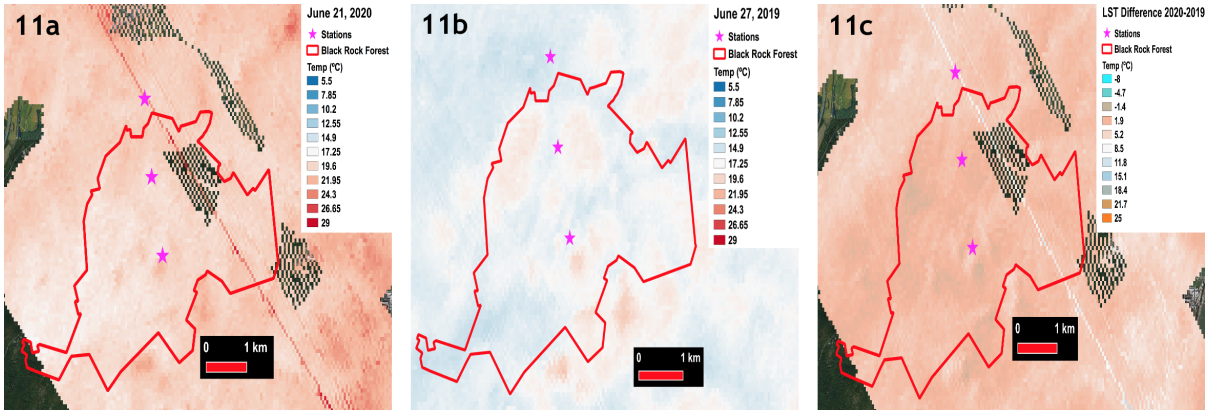

Figure 11: a) LST on 21 June 2020, local time 7:31am b) LST on 27 June 2019, local time 6:07am c) LST difference image (21 June 2020 – 27 June 2019) with a temperature difference scale ranging from -8° to 25°C

3.2.2 LST Patterns

Temperature patterns are key in analyzing frost damages and forest health. The satellite data collected by the ECOSTRESS sensor provides LST information over a period of time. Temperature patterns in 2020 show a steady rise in LST from the end of May towards the end of June, with the lowest LST reading on 21 May 2020 (See Figure 12a and Table 1). Temperature patterns in 2019 show fluctuations in LST from end of May to end of June, with the lowest LST reading on 13 June 2019 (See Figure 12a and Table 1). To ensure that our readings are accurate, temperature sensors were installed in the following three stations of BRF: 1.) Fire Tower Station, representing readings from the highest point of elevation 2.) Lowland Station, representing readings from the lowest point of elevation and 3.) Ridgetop Station. The LST readings from different stations (Figure 12b) confirm the mean LST readings of BRF (Figure 12a).

Table 2. *ECOSTRESS LST Statistics of Black Rock Forest for years 2020 and 2019*

Data number	Pixel count	Minimum temperature [ºC]	Maximum temperature [ºC]	Mean temperature [ºC]	std	Year	DOY	Date	Mean anomaly	edt
0	4142	34.45	50.41	41.624645	3.5877354	2020	111	20-Apr-2020	1.79119548	7:54
1	4130	8.33	14.13	10.78237	0.9323978	2020	142	21-May-2020	0.46398792	20:08
2	4131	15.35	21.59	17.300215	0.8223121	2020	165	13-Jun-2020	0.74446441	10:40
3	4135	17.15	28.27	19.493994	0.9580865	2020	173	21-Jun-2020	0.83886731	7:31
4	4136	24.93	31.87	26.991133	0.94525087	2020	177	25-Jun-2020	1.16148487	12:25

Data number	Pixel count	Minimum temperature [ºC]	Maximum temperature [ºC]	Mean temperature [ºC]	std	Year	DOY	Date	Mean anomaly	edt
0	4141	11.67	14.85	13.039299	0.5186532	2019	145	25-May-2019	0.56110829	18:50
2	4133	22.65	31.15	24.37194	0.75741434	2019	159	8-Jun-2019	1.04877552	13:45
3	4138	11.61	15.65	13.097895	0.63431394	2019	160	9-Jun-2019	0.5636298	19:24
4	4138	6.29	9.31	7.383989	0.36800674	2019	164	13-Jun-2019	0.31774848	17:43
5	4130	14.09	19.93	16.823648	0.8747954	2019	178	27-Jun-2019	0.72395674	6:07

3.2.3 LST and Elevation

Field measurements from the three stations indicate the highest temperature readings from the Fire Tower Station for both years (See Figure 12b). This leads us to conclude that higher elevation shows warmer temperatures compared to the other stations. Further observations are required to confirm this observation.

3.2.4 Factors that Affect Data Loss and Anomalies

The amount of useful data depends on pixels that give the accurate reading of LST. Clouds, for example, alter the accuracy and create huge anomalies in LST readings. In order to prevent cloud anomalies, a python program was written to create a cloud mask removing all the pixels in the images that represent clouds. Due to the abnormally low temperatures and the presence of clouds in the atmosphere, many of the pixels were taken out of our raw satellite images which resulted in a significant loss of ECOSTRESS LST data. Clouds are not the only culprit for data loss. Signal disruption due to solar panels also affected the quality of the images taken by the sensor. On 20 April 2020, a mean LST reading of 42ºC was recorded in BRF (See Table 2). This particular reading is an error since Accuweather.com records an average temperature of 13ºC on this date. This anomaly could be the result of sensor or equipment malfunction. After the frost date or 9 May 2019, LST patterns vary and the anomalies are recorded in Figure 12c.

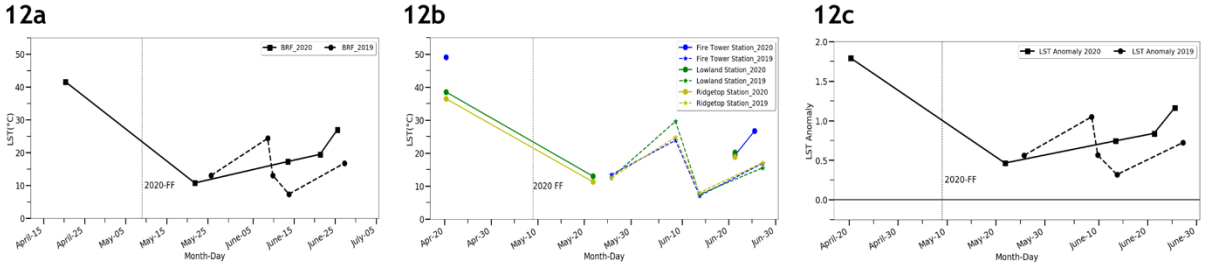

Figure 12. a) Comparison of ECOSTRESS LST of Black Rock Forest from mid-April to end of June for years 2020 and 2019 b) ECOSTRESS mean LST values taken at the Lowland, Ridgetop and Fire Tower Stations from mid-April to end of June for years 2020 and 2019 c) Measurement of anomalies in LST of Black Rock Forest from mid-April to end of June for years 2020 and 2019

3.3 NDVI and LST

Our NDVI findings reflect the frost damages and the forest recovery in 2020. Our LST findings show us a variation of temperature and serve as a guide in understanding the health of the forest during and after the frost. Using the measurements of LST and NDVI is an effective tool in defining the effects of late spring frosts in temperate deciduous forests. There is still plenty of research and improvements to be done on using the ECOSTRESS sensor for a more efficient method in studying LST.

4. DISCUSSION AND CONCLUSIONS

The Landsat-8 NDVI images of 2019, where there was no frost event, show consistency in the rise of forest greenness from early May to beginning of June. NDVI images of 2020 before the frost event shows similarities in greenness with 2019. Mean NDVI values show a steady level of forest greenness from early 2020 until 3 May 2020, with a mean NDVI value of 0.4. NDVI values significantly decrease right after the frost event as indicated by the NDVI image from 12 May 2020. The recorded NDVI on 4 June 2020 with a mean value of 0.8 indicates canopy recovery, approximately 26 days after the frost event.

Weather station data confirms the hard freeze on 9 May 2020. LST highlights the cooler temperatures of the forest compared to urban areas. Due to the presence of clouds, ECOSTRESS LST during low temperatures are scarce and we were not able to observe the LST before 9 May 2020 and 9 May 2019. LST analyses after 9 May in both years show a steady rise in temperature, including warmer values after late June in 2020, and a fluctuating pattern in temperature in 2019. The warmer measurements of 2020 in mid-April show a high level of anomaly that could be attributed to sensor malfunction. Our preliminary investigations require further study to compensate the data loss as a result of removed pixels with cloud content. Further research will be conducted to ascertain the reasons for such anomalies in temperature and whether ECOSTRESS LST can accurately reflect late spring frost effects.

5. FUTURE WORK

Further research will be conducted on the diurnal temperature range, as well as the vegetation water content. To compare and verify the vegetation water content the NDVI values from MODIS will be plotted and compared. The negative correlation between the soil moisture and surface temperature provided us with little information and will need to be further analyzed. The coherence needs to be computed and further analyzed in order to understand its significance.

6. ACKNOWLEDGMENTS

This project is supported by the National Science Foundation Research Experiences for Undergraduates (Grant # 1950629), under the direction of Dr. Reginald A. Blake, Dr. Janet Liou-Mark, and Ms. Julia Rivera.

The authors are grateful for the support from The National Oceanic and Atmospheric Administration – Cooperative Science Center for Earth System Sciences and Remote Sensing Technologies (Grant # NA16SEC4810008) under the direction of Dr. Shakila Merchant. The authors are solely responsible for the content of this article, and it does not necessarily represent the views of the NSF CREST REU.

7. REFERENCES

1. Augspurger, C. K. [2009]. Spring 2007 warmth and frost: Phenology, damage and refoliation in a temperate deciduous forest. Functional Ecology, 23(6), 1031-1039. https://doi.org/10.1111/j.1365-2435.2009.01587.x

2. Augspurger, C. K. [2013]. Reconstructing patterns of temperature, phenology, and frost damage over 124 years: Spring damage risk is increasing. Ecology, 94(1), 41-50. https://doi.org/10.1890/12-0200.1

3. Hayhoe, K., Wake, C. P., Huntington, T. G., Luo, L., Schwartz, M. D., Sheffield, J., Wood, E., Anderson, B., Bradbury, J., DeGaetano, A., Troy, T. J., & Wolfe, D. [2006]. Past and future changes in climate and hydrological indicators in the US Northeast. Climate Dynamics, 28(4), 381-407. https://doi.org/10.1007/s00382-006-0187-8

4. Rafferty, J. P. (2019, March 27). Frost. Retrieved August 24, 2020, from https://www.britannica.com/science/frost-meteorology

5. Verhoeven, G. J. (2011, March 25). Near-Infrared Aerial Crop Mark Archaeology: From its Historical Use to Current Digital Implementations. Retrieved August 24, 2020, from https://link.springer.com/article/10.1007/s10816-011-9104-5

6. Vitasse, Y., Lenz, A., & KÃ¶rner, C. [2014]. The interaction between freezing tolerance and phenology in temperate deciduous trees. Frontiers in Plant Science, 5. https://doi.org/10.3389/fpls.2014.00541